Journal of Alloys and Compounds, 195 (1993) 731–734
JALCOM 7569

Low Power High Speed Rotor (200 000 rpm) with HTSC Bearings

V. V. Nemoshkalenko and B. G. Nikitin

Institute of Metal Physics, 252680 Kiev, Ukraine

Abstract

A self-stabilized magnetic rotor running on bearings of the high temperature superconductor (HTSC) $YBa_2Cu_3O_{7-\delta}$ with a rotational speed of about 79 000 rpm in air and of about 200 000 rpm in vacuum of 10^{-2} torr at a power consumption of about 3.1 mW is described. The energy losses due to the interaction of the magnetic rotor with air at various pressures, with a superconductor and with an amorphous soft ferromagnetic powder have been studied. Some physical parameters determining magnetic rotor–medium interaction were obtained as well.

1 Introduction

It is known, that a permanent magnet can levitate above a high temperature superconductor in a stable configuration [1,2].

Theoretical models for describing the levitation forces have been given in refs. [1,3]. In ref. [4], the dynamics of a permanent magnet levitating above a high temperature superconductor was investigated and the ranges of both the hysteretic and quasi-elastic losses were determined. The results presented in [3,4] are of particular interest, as they can be used for constructing a magnetic rotor running with high speed on superconducting bearings virtually without magnetic friction.

Besides its application in constructing gyroscopes, sensitive vibration sensors and natural-damping accelerometers, the magnetic rotor can be used in various branches of experimental physics, for example for measuring the magnetic friction in both the quasi-elastic and hysteretic ranges [5], for investigating magnetic flux creep [4], or for determining the viscosity of gases and liquids at cryogenic temperatures.

When compared with the traditional constructions [6,7], the rotor considered here has a number of advantages due to its rotation self-stabilization, rapid damping of nutation oscillations when driven and the low energy requirements of the suspension system.

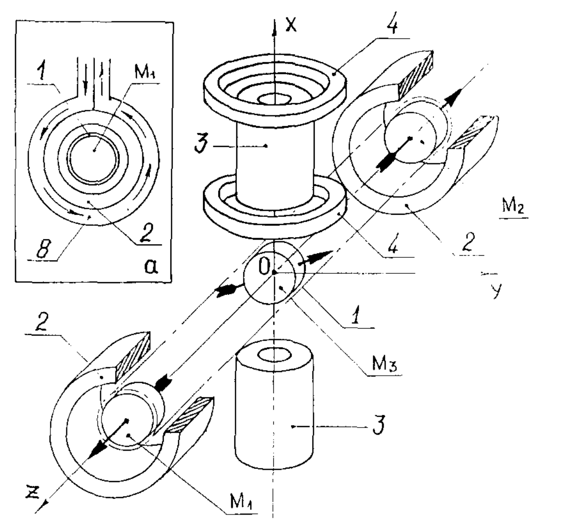

Fig. 1. Schematic drawing of the high-speed magnetic rotor with superconducting bearings. M_1, M_2, M_3: Sm-Co magnets (direction of moment shown by arrows), 1: plastic tube, 2: $YBa_2Cu_3O_{7-\delta}$ high temperature superconductor, 3: driving coils, 4: detection coils. For clarity, the outer cylinder is not shown. Insert: Schematic drawing of the liquid nitrogen cooling (8) of the high temperature superconductor.

2 Description of the magnetic rotor

Fig. 1 shows a schematic of the high-speed magnetic rotor with superconducting bearings. The magnetic rotor consists of two Sm-Co magnet disks (M_1 and M_2) with a thickness of 2 mm and a diameter of 4 mm. The magnetic moments are directed along the z-axis pointing in opposite directions for mirror symmetry. The magnets M_1 and M_2 are used to suspend the rotor in cylindrical superconducting $YBa_2Cu_3O_{7-\delta}$ bearings (2) with inner and outer diameters of 10 mm and 26 mm and a width of 9 mm. The magnet M_3 is used for driving the magnetic rotor and for determining its rotational speed. The rotor is running inside a thin stationary cylinder with 10 mm inner diameter; this outer cylinder is not shown in Fig. 1.

Fig. 2 shows an x-y section of the device for driving the rotor around its symmetry axis z. There are two identical driving coils (3) with 500 turns each, connected in series, and two coils (4) to record the rotor speed ν.

0925-8388/93/$06.00

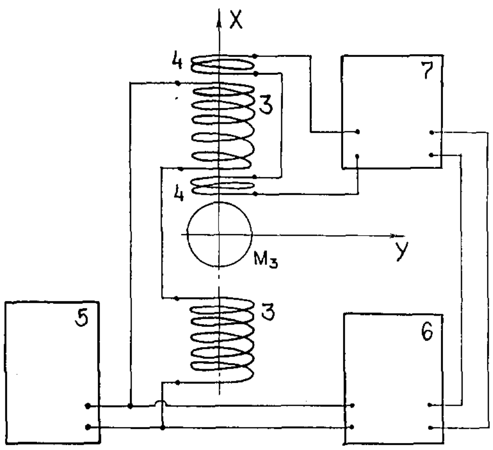

Fig. 2. Schematic diagram of the drive unit for the magnetic rotor. M_3: Sm-Co magnet, 3: driving coils, 4: detection coils, 5: audio-signal generator, 6: oscilloscope, 7: amplifier.

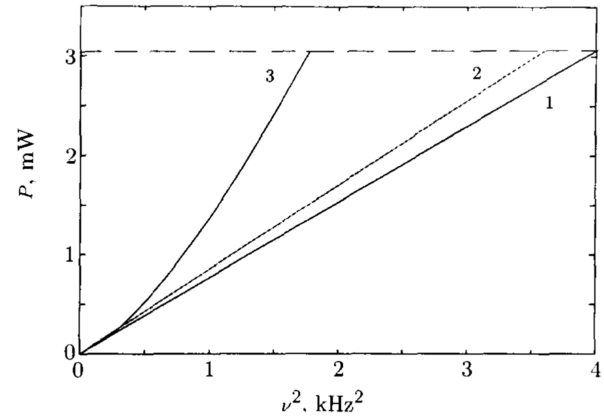

Fig. 3. The power consumption P of the rotor *vs* square of the rotation frequency ν^2 in vacuum of 10^{-2} torr (1), 10^{-1} torr (2), and in air (3).

To determine the power consumption P of the rotor, the phase difference α between the driving field $H = H_0 \cos(2\pi\nu t)$ generated by the coils (3) and the signal induced in coils (4) was measured (see Fig. 2). The amplitude H_0 was determined by a Hall sensor through which a constant current was passed which had the same amplitude as the variable current through coils (3). The power consumption was calculated through

$$P = \nu \int_0^{2\pi} \left| \vec{M} \times \vec{H} \right| d\varphi = \pi\nu M H_0 \left|\cos\alpha\right| \qquad (1)$$

where $\vec{M}$ is the magnetic moment of M_3, φ is the angle between $\vec{M}$ and the x-axis, ν is the rotation frequency and the phase angle α can depend on ν. The estimated error of P amounts to about 10% at $P = 1$ mW.

The best magnetic rotors used in this work with small misorientations ($\approx 0.3°$) between the magnetic moments M_1 and M_2 and the free rotor axis of inertia will be called "perfect" below. Rotors made especially with misorientations of $\approx 3°$ will be called "imperfect". In this paper, we present only results on "perfect" rotors.

3 Analysis of energy loss due to rotor–medium interaction

Fig. 3 shows the experimental dependence of the power P consumed by the "perfect" rotor on the square of the rotation frequency ν^2 in a vacuum of 10^{-2} and 10^{-1} torr and in air of ambient pressure (curves 1, 2, and 3) for the system described above. As follows from theory [8], the quadratic dependence of P on ν^2 allows us to conclude that the rotation of the magnetic rotor in vacuum is accompanied by viscous friction within the whole frequency range under consideration (curves 1, 2 in Fig. 3). In air, a quadratic dependence is observed up to $\nu \leq \nu_0 = 3.3 \times 10^4$ rpm, but at $\nu > \nu_0$, the power consumption increases more rapidly with $P \sim \nu^{2.8}$ which testifies to the appearance of turbulence [9].

On the basis of the experimental data (Fig. 3) within the frequency ranges where $P \sim \nu^2$ (laminar flow regime) for a cylinder rotating inside a fixed one, the values of the viscosity η in various media were determined according to [8]

$$\eta = \frac{1}{16\pi^2} \cdot \frac{P}{\nu^2} \cdot \frac{R_{ext}^2 - R_{int}^2}{l \cdot R_{ext}^2 \cdot R_{int}^2} \qquad (2)$$

where $l = 2$ cm is the length of the cylinders, $R_{int} = 0.2$ cm and $R_{ext} = 0.5$ cm are the radii of the inner (rotor) and the external cylinder, respectively. The values for the viscosity of air at reduced pressure were obtained as follows $\eta(10^{-1}\text{ torr}) = 1.8 \times 10^{-4}$ g/s cm and $\eta(10^{-2}\text{ torr}) = 1.6 \times 10^{-4}$ g/s cm. These values agree with published values [10] of the viscosity. This confirms that other contributions towards losses, including vortex depinning, are negligible.

Thus, from the experimental data (Fig. 3) we can conclude that there is no essential vortex depinning at rotation of the "perfect" rotor, *i.e.* the very small power consumption takes place owing to magnetic losses of the quasi-elastic type [4, 5]. This opens the possibility to achieve 200 000 rpm already in a vacuum of 10^{-2} torr at a power consumption of about 3 mW. A further increase of the rotational speed was not carried out in the present work for lack of a generator with smooth frequency change within a single interval from 0 Hz to above 3000 Hz.

The energy loss due to the interaction of the magnetic rotor with an amorphous soft magnetic powder (FC 139, powder size 1.3μm, resistivity about 10^{-6} Ωcm) was also determined in this work. A contribution to the losses due to the hysteresis and magnetic viscosity is also discussed. For this purpose, two cylinders of 6 mm in diameter and 18 mm in length, made from the FC 139-type material, were placed inside the driving coils (3) at a distance of 4 mm from the rotor axis. Then the decrease of the rotation frequency ν was determined as a function of time after switching off the driving field.

Taking into account a linear dependence $\nu(t) = \nu_0 - a\,t$, the hysteresis losses W were estimated according to the relation $a = W/(2\pi I)$, where $I = \frac{1}{2} m R_{int}^2$ is the moment of inertia of the rotor, and m and R_{int} are its mass and radius. The Q-factor of the system was determined as $Q = 2\pi W_0/W = 4\pi^3 I \nu^2/W$, where W_0 is the rotation energy of the rotor at the frequency of $\nu = 2000$ Hz. According to the estimates obtained, we have $W = 1.76 \times 10^{-5}$ J, which is in agreement with the result of ref. [11], $Q = 4.5 \times 10^4$.

References

1 V. V. Nemoshkalenko, M. A. Ivanenko, B. G. Nikitin, Yu. G. Pogorelov, and G. A. Klimenko, Preprint 6.89, Institute of Metal Physics, Kiev (1989) (in Russian).

2 V. V. Nemoshkalenko, M. A. Ivanenko, and B. G. Nikitin, Metallofizika **11** (1989) 124.

3 V. V. Nemoshkalenko, M. A. Ivanenko, B. G. Nikitin, Yu. G. Pogorelov, and G. A. Klimenko, Solid State Commun. **7** (1990) 637.

4 V. V. Nemoshkalenko, E. H. Brandt, A. A. Kordyuk, B. G. Nikitin, and Yu. G. Pogorelov, Physica C **170** (1990) 481.

5 V. V. Nemoshkalenko, M. A. Vasil'ev, M. A. Ivanov, A. A. Kordyuk, B. G. Nikitin, and Yu. G. Pogorelov, Superconductivity: Physics, Chemistry, Technique **3** (1990) 2751 (in Russian).

6 Yu. G. Martinenko, Motion of Solid State in Electrical and Magnetic Fields, Moscow: Nauka (1988) (in Russian).

7 J. T. Harding, Report No. 345-8, Jet Propulsion Lab., California Institute of Technology (1964).

8 L. D. Landau and E. M. Lifshitz, Hydrodynamics (Course of Theoretical Physics, Vol. VI), Oxford: Pergamon (1980).

9 G. I. Taylor, Phys. Trans. A **223** (1923) 289.

10 L. N. Rozanov, Vacuum Technics, Moscow: Visshaya Shkola (1982) (in Russian).

11 Amorphous Alloys, Moscow: Metallurgiya (1984) (in Russian).